Impact of Frequency-Hopping NB-IoT Positioning in 4G and Future 5G Networks

José A. del Peral-Rosado, José A. López-Salcedo, and Gonzalo Seco-Granados
Universitat Autònoma de Barcelona (UAB), Bellaterra, Spain
Email: {JoseAntonio.DelPeral, Jose.Salcedo, Gonzalo.Seco}@uab.cat

***Abstract*—The positioning support is under study within the narrowband (NB) Internet of things (IoT) standard of Long Term Evolution (LTE) cellular networks. However, the limited signal bandwidth of this technology poses serious difficulties to achieve a position accuracy below 50 meters, which may be required in current 4G and future 5G standards. This work studies the impact of a frequency-hopping (FH) scheme on the LTE positioning reference signal (PRS) for NB-IoT applications. The downlink time-difference of arrival (TDoA) method is used to compute the achievable positioning performance of FH PRS scheme. The simulation results indicate the feasibility to achieve a position accuracy below 50 meters, by covering a system bandwidth of 10 MHz with two consecutive hops. Future work is aimed to evaluate the FH impairments for advanced configuration schemes.**

I. Introduction

Internet of things (IoT) applications are expected to have a huge growth within the following decade. Many devices nowadays operating stand-alone are going to be connected with a wireless network. The most traditional communication solutions are based on the use of short-range technologies, such as ZigBee or Bluetooth. But, the introduction of long-range and low data rate technologies, such as SigFox or LoRa, is allowing the development of new IoT services, such as float management, asset tracking or Smart Cities applications [1]. In order to complement these proprietary technologies and to cover the IoT market growth, the Third Generation Partnership Project (3GPP) has initiated the standardization of IoT solutions within current fourth-generation (4G) and future fifth generation (5G) of cellular networks.

The specification of the narrowband IoT (NB-IoT) solution within the Long Term Evolution (LTE) standard is of special interest. This feature may allow the mobile devices to cope with the stringent IoT requirements, such as a long battery life (above 10 years), low power consumption, and long-range communication coverage. These features make the NB-IoT technology a good candidate for the initial 5G standardization of IoT solutions.

The 3GPP standard is also studying the support of NB-IoT positioning within Release 14 [2], since the location information is known to provide enhancements on the communication performance [3]. Although there are no definite positioning requirements, a position accuracy of 50 meters in indoors and outdoors, i.e., required in [4], is generally adopted as a initial target. This accuracy requirement poses a tremendous challenge for NB-IoT positioning in dense multipath, especially for those methods based on time-difference of arrival (TDoA) measurements, due to the very low signal bandwidth used. In order to circumvent the low-bandwidth problem, several solutions have been proposed in the literature for other technologies, such as a round-trip time solution for WiFi in [5] or a frequency-hopping (FH) solution for the Global System for Mobile communications (GSM) in [6]. Indeed, the 3GPP consortium has proposed the introduction of a FH scheme for NB-IoT positioning, such as in [7], [8] and [9]. However, the coherent approach of this scheme has not been studied. Thus, the objective of this work is to discuss the impact of coherent FH positioning within NB-IoT applications, and to provide insights on its achievable positioning performance.

The remainder of this paper is organised as follows: Section II introduces the current status of narrowband positioning within the 3GPP standard, Section III describes a widely-adopted multipath mitigation technique to compute ranging measurements, Section IV discusses the FH NB-IoT scheme and its main limitations, Section V assesses the simulation results, and Section VI draws the conclusions and future work.

II. 3GPP Narrowband Positioning

A. Standardization of Cellular IoT

The number of IoT applications is expected to substantially increase in the following years, due to a growing demand of connectivity from low-cost and low-energy devices. Since this demand may not be only covered by existing proprietary technologies operating in unlicensed bands, the 3GPP consortium has developed standard cellular technologies in order to offer IoT services in current licensed bands. As it is summarized in Table I, three main cellular IoT solutions has been introduced in the 3GPP standards [2]:

1) eMTC: The LTE standard was first adapted to machine-type communications (MTC) with the introduction of LTE-M in Release 12. This specification is based on a user equipment (UE) category with low requirements, called LTE Cat 0. These low requirements are based on half-duplex and single-antenna transmissions with a power up to 23 dBm, in order to achieve a throughput up to 1 Mbps. In Release 13, the LTE-M is further optimized with eMTC, which introduces LTE Cat M1. This UE category reduces the signal bandwidth to 1.08 MHz or six resource blocks (RBs), which is the minimum LTE resource allocation formed by 12 subcarriers of 15 kHz and 7 orthogonal frequency division multiplexing (OFDM) symbols.

2) NB-IoT: Further IoT enhancements were introduced with NB-IoT in Release 13 of LTE, which defines LTE Cat M2. The signal bandwidth is reduced to 180 kHz (or one RB) and the downlink throughput is up to 250 kbps. The NB-IoT solution can be deployed with three different operation modes: stand-alone, in-band LTE and guard-band LTE. The first mode

TABLE I. CELLULAR IOT TECHNOLOGIES IN 3GPP STANDARDS.

3GPP technology	Deployment	Signal bandwidth	Power Class
eMTC	In-band LTE	1.08 MHz	20 / 23 dBm
NB-IoT	In-band and guard-band LTE, and stand-alone	180 kHz	23 dBm
EC-GSM-IoT	In-band GSM	200 kHz	23 / 33 dBm

uses a narrowband carrier of 200 kHz allocated for the NB-IoT operation, such as dedicated narrowband carriers or re-farmed GSM bands. The in-band and guard-band modes allocate the NB-IoT resources in available spots of a LTE carrier, or in the unused guard bands, respectively.

3) EC-GSM-IoT: The GSM standard is enhanced for IoT services in Release 13, by introducing the EC-GSM (extended coverage GSM) operation mode. The aim of this mode is to enhance the link budget by 20 dB, in order to cover devices suffering deep signal attenuation, such as sensors and meters located in basements.

B. Standard Narrowband Positioning

The positioning support within the cellular narrowband technologies is under study in Release 14. The objective is to partially adopt some of the LTE positioning methods specified in [10] with minimum changes to the current narrowband specification. Given the limitation of communications resources and reduced device complexity, the positioning support is now restricted to the E-CID, observed TDoA (OTDoA) and uplink TDoA (UTDoA) methods. The evolution of each of these technologies is discussed in different work items:

1) Further Enhanced MTC for LTE: The further study of E-CID and OTDoA positioning methods for eMTC is proposed in [11]. The OTDoA enhancements are mainly focused on the transmission of multiple PRS time-frequency configurations, and the support of PRS frequency hopping [12].

2) Enhancements of NB-IoT: The support of positioning methods within NB-IoT is studied in [13]. The legacy positioning reference signal (PRS) used within the OTDoA method is adapted for NB-IoT, by specifying the narrowband PRS (NPRS) allocated over one RB within the time-frequency grid. The frequency-hopping NPRS allocation is proposed in [7] and [8], where the receiver is assumed to be re-tuned at each narrowband [9]. The use of the uplink access channel for UTDoA narrowband measurements is under study [12].

3) Positioning Enhancements for GERAN: The positioning enhancements within GSM EDGE Radio Access Network (GERAN) are studied in [14], by targeting a position accuracy of EC-GSM-IoT devices better than 100 meters. The multilateration of timing advance and observed time difference measurements has been introduced within this work item [15].

III. MULTIPATH MITIGATION

Multipath is one of the main challenges to achieve accurate ranging measurements for TDoA-based positioning in urban environments, due to the high number of reflections and obstructions of the line-of-sight (LoS) between base station (BS) and mobile device. Thus, multipath mitigation techniques are necessary in order to reduce the induced ranging bias. However, the use and performance of these techniques is limited in IoT applications due to the reduced power consumption and low signal bandwidth available. Thus, only low-complexity algorithms may be applied within IoT sensors. This section describes a well-known time-delay estimator able to counteract or reduce the effect of multipath under certain conditions, which are also discussed.

A. First-peak or Threshold-based Estimator

A widely-adopted ranging estimator is based on the first peak of the cross-correlation (between the received and pilot signals) above a certain threshold [16], which is typically called first-peak or threshold-based estimator. This estimator is mainly characterized by its low computational complexity, and it is widely adopted by the 3GPP community for OTDoA performance evaluation.

Considering a fine frequency synchronization, the received OFDM pilot signal is written in the frequency domain for the n-th subcarrier as

$$r\left(n\right) = H\left(n\right) b\left(n\right) e^{j\frac{2\pi\tau n}{N}} + w\left(n\right), \tag{1}$$

where $H\left(n\right)$ is the channel frequency response, $b\left(n\right)$ is the pilot signal, N is the total number of in-band subcarriers, τ is the time delay, and $w\left(n\right)$ is the additive white Gaussian noise (AWGN) contribution, i.e., $w\left(n\right) \sim \mathcal{CN}\left(0, \sigma_{\mathrm{W}}^2\right)$. Then, threshold-based time-delay estimation (TDE) is defined as [17]

$$\hat{\tau} = \min_{\tau_{\min} \leq \tau < \tau_{\max}} \left\{\tau\right\} \quad \text{s.t.} \quad \Lambda\left(\tau\right) \geq \Lambda_{\mathrm{thr}}, \tag{2}$$

where $\tau_{\min}$ and $\tau_{\max}$ is the minimum and maximum estimation value, respectively, Λ_{thr} is the likelihood threshold, and the likelihood function is

$$\Lambda\left(\tau\right) = \left|\sum_{n\in\mathcal{N}} r\left(n\right) b^{*}\left(n\right) e^{-j\frac{2\pi n\tau}{N}}\right|^2, \tag{3}$$

being $\mathcal{N}$ the set of subcarrier indexes of the pilot signal. The estimation range should be adequately defined according to the accuracy of the signal synchronization. For instance, if there is a fine synchronization, the estimation range can be reduced to the sampling period. The threshold Λ_{thr} can be computed with several methods described in [17], or designed heuristically, e.g.

$$\Lambda_{\mathrm{thr}} \simeq \Lambda_{\max}/4, \tag{4}$$

where $\Lambda_{\max}$ is the maximum of the likelihood function $\Lambda\left(\tau\right)$.

B. Performance Limits

The main performance limits of the threshold-based estimator are the non-LoS (NLoS) conditions and the resolvability of the multipath reflections [16]. The lack of LoS introduces a ranging bias, which cannot be counteracted by this estimator. Nonetheless, resolvable multipath components allow the correct identification of the LoS correlation peak, in order to achieve an accurate TDE. The resolvability of the multipath reflections depends on the signal bandwidth, i.e., the multipath resolvability is higher with a high signal bandwidth. Thus, the use of narrowband signals is expected to result in a poor TDE performance. As it is discussed in the following section, the TDE performance may be enhanced by virtually increasing the signal bandwidth with a FH allocation of the narrowband PRS.

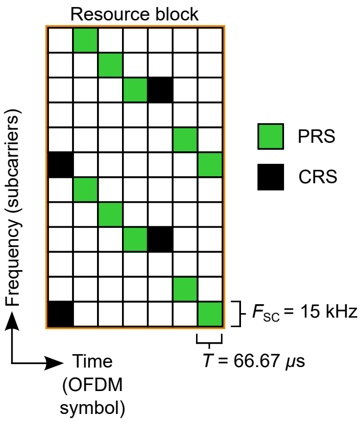

Fig. 1. Allocation pattern of the CRS and PRS within one RB.

IV. Frequency-Hopping NB-IoT Positioning

Dense multipath is expected to prevent high-accuracy positioning with narrowband signals. As a potential solution, the coherent TDE of FH narrowband signals may increase the achievable ranging capability in multipath environments. This section describes the FH approach with one-RB PRS for NB-IoT positioning, and its main limitations.

A. Frequency-Hopping PRS of One RB

The allocation pattern of the cell-specific reference signal (CRS) and PRS within one RB is shown in Figure 1, by considering a slot without control signals. The PRS is distributed over ten different subcarriers and five out of seven OFDM symbols over one slot. Since the subcarrier spacing is $F_{\text{sc}} = 15$ kHz, the OFDM symbol period is $T = 1/F_{\text{sc}} = 66.67\mu$s. Then, the resource elements of the PRS can be grouped within one symbol. Assuming fine frequency synchronization and low receiver dynamics over one slot, this grouped PRS symbol is expected to result in a improved TDE accuracy with respect to the use of only one PRS symbol.

The ranging performance can be further enhanced by hopping the NB-IoT allocation of the PRS over different slots and subcarriers, while preserving a coherent TDE. Considering the same assumptions as for one RB, the PRS resource elements of different hops can also be grouped into one symbol, as it is shown in Figure 2. Assuming a coherent TDE of the grouped FH symbol, the ranging performance is enhanced for a wide bandwidth allocation between hops. In this sense, a FH narrowband signal allocated over a large bandwidth may achieve accurate ranging estimation even in dense multipath environments. However, depending on the receiver architecture, a phase offset and group delay may be introduced for each hop of the PRS. Thus, the ranging performance of a fully coherent TDE may not be achieved. In the worst-case scenario, these receiver impairments between hops may result in a non-coherent TDE, which only achieves the integration gain of the accumulated hops. Let us approximate the received grouped FH PRS symbols in the time-domain as

$$x\left(m\right) = \sum_{k=1}^{K} \sum_{n \in \mathcal{N}_k} H\left(n,k\right) b\left(n,k\right) e^{j\theta_k} e^{j\frac{2\pi n\left(m-\tau+\Delta_k\right)}{N}} + w\left(m\right), \tag{5}$$

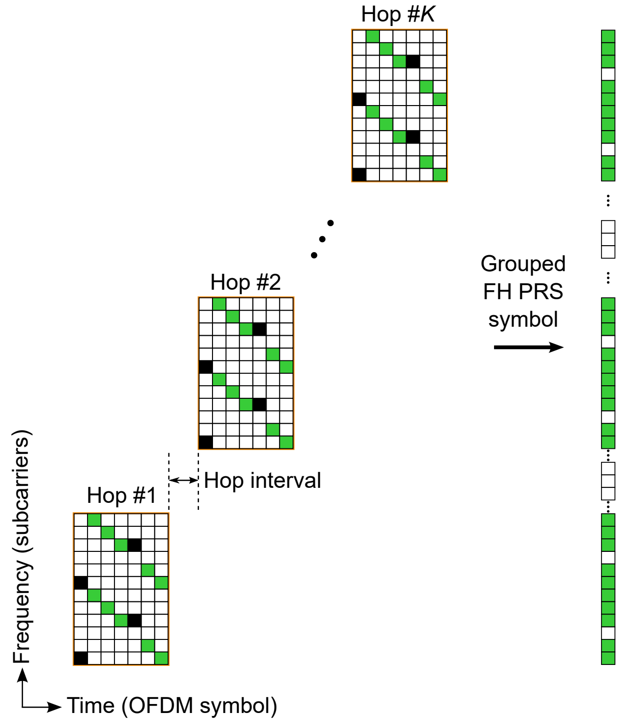

Fig. 2. Allocation scheme of the FH PRS for NB-IoT positioning.

where θ_k is the phase offset for the k-th hop, Δ_k is the group delay for the k-th hop, and $\mathcal{N}_k$ is the set of PRS subcarrier indexes for the k-th hop from a total of K hops.

B. Limitations of Coherent Frequency-Hopping Positioning

The coherent FH PRS is aimed to achieve a positioning accuracy similar to the use of PRS measurements over a wideband transmission of the equivalent signal bandwidth, by means of a coherent TDE. However, four main impairments are likely to limit this achievable positioning accuracy:

1) Signal Acquisition and Tracking: Fine time and frequency synchronization of the signal is necessary to remove the clock offset of the mobile device. Although this synchronization error is assumed to be negligible in (1) and (5), a residual clock offset during the signal acquisition and tracking can result in a ranging error after the integration of several PRS slots. Thus, a high hop interval may increase the impact of this residual clock offset.

2) Hop Impairments: The phase offset and group delay at each hop introduce a bias on the TDE. These impairments mainly depend on the receiver architecture. For instance, the re-tuning of the receiver front-end to each narrowband may introduce a random phase offset and specific group delay.

3) Dynamics: The variation of the time delay due to the dynamics of the mobile device results in a ranging error. In addition, these dynamics reduces the coherence time of the multipath channel, which also introduces a bias on the TDE of the grouped FH PRS symbol. Thus, the device dynamics limit the integration time and the maximum hop interval, and as a result, the number of hops.

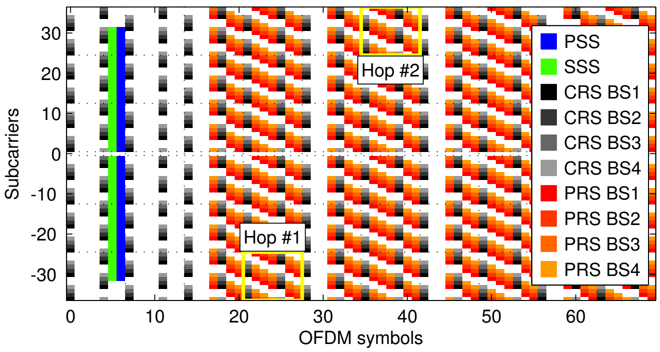

Fig. 3. Two hops over an in-band PRS transmission of 6 RB.

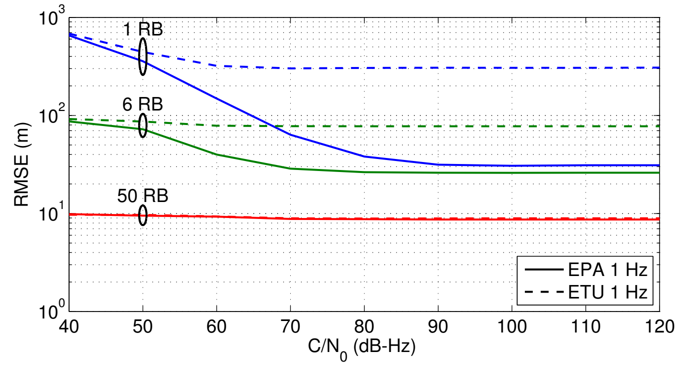

Fig. 4. RMSE of a threshold-based estimator for narrowband PRS of one RB and the FH PRS covering 6 RB and 50 RB, by using 1000 Monter-carlo simulations.

4) Cross-correlation sidelobes: The sparse allocation of one-RB PRS hops in the frequency-domain results in an increase of the sidelobes of the cross-correlation function. Thus, a ranging error may be incurred by estimating the time delay of the cross-correlation sidelobe, instead of the time delay of the main lobe, resulting in a detection ambiguity [18]. This limits the frequency separation between hops.

V. Performance Results

The objective of this section is to evaluate the achievable ranging and positioning performance of coherent FH NB-IoT with minimum PRS resources. For this purpose, the FH scheme of the narrowband PRS consists of two hops of one RB in two consecutive subframes, where only two PRS slots are used (i.e., hop interval of 0.5 ms). An in-band PRS transmission of 6 RB (1.08 MHz) and 50 RB (8.94 MHz) is considered, and only one RB at each edge of the band is used in the FH approach to coherently estimate the time delay over the maximum bandwidth. For instance, the coherent FH TDE is shown in Figure 3 for 6 RB and four tightly-synchronized BSs.

The mobile device is considered to be almost static with a Doppler shift equal to 1 Hz. In order to consider a multipath channel with low and high delay spread, the standard extended pedestrian A (EPA) and extended typical urban (ETU) channel models are used, respectively, whose specification can be found in [19]. A fine synchronization of the signal is assumed before starting the computation of the FH PRS measurements. Thus, the threshold-based estimator is defined with the heuristic threshold in (4), and the estimation range is set by $\tau_{\min} = -T_{\rm s}/2$ and $\tau_{\max} = T_{\rm s}/2$, where $T_{\rm s} = T/N$ is the sampling period. In these conditions, the main FH impairments are based on a certain phase offset and group delay between hops.

A. Impact on the Ranging Performance

The ranging performance of the threshold-based estimator is assessed for the narrowband PRS of one RB, and the FH PRS covering 6 RB and 50 RB of signal bandwidth with two hops. First, the root-mean-square error (RMSE) of the TDE is computed as a function of the carrier-to-noise ratio (C/N_0) by considering no hop impairments for the EPA and ETU multipath channels with 1000 Monte-carlo simulations. As it is shown in Figure 4, the RMSE is below 50 meters for $C/N_0 \geq 90$ dB-Hz with any of the simulated configurations over the EPA channel, while the FH PRS covering 50 RB of signal bandwidth is required to achieve this accuracy over the ETU channel. This is due to the dense multipath and high delay spread of the ETU channel (i.e., 5 μs) with respect to the low delay spread of the EPA channel (i.e., 410 ns).

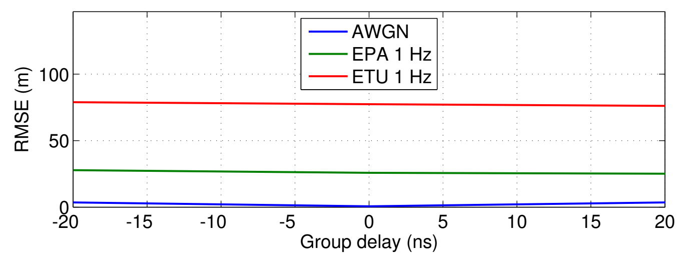

(a) 6 RB

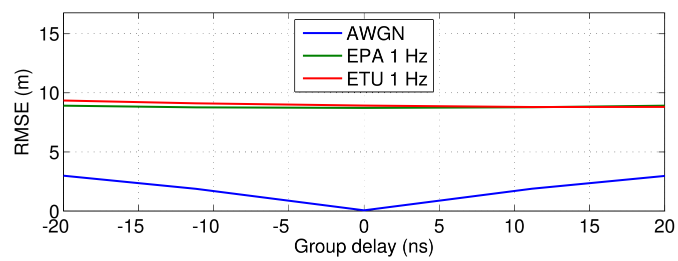

(b) 50 RB

Fig. 5. Impact of the group delay on the RMSE of the TDE with two hops over 6 and 50 RB for C/N_0 =90 dB-Hz without phase offset, i.e., $\theta_k = 0$, by using 1000 Monter-carlo simulations.

Let us assume a $C/N_0 = 90$ dB-Hz to assess the impact of the hop impairments. First, a group delay between -20 ns and 20 ns is introduced without any phase offset. The resulting RMSE is shown in Figure 5 for AWGN, EPA and ETU channels. As it can be seen, the group delay assumed in these simulations has a limited impact on the RMSE of the TDE. Second, a phase offset between $-\pi$ and π is introduced without any group delay. As it shown in Figure 6, a high phase offset may result in a considerable ranging error, due to the loss of coherency on the TDE within the grouped FH PRS symbol. Thus, the architecture of the NB-IoT receiver should be designed accordingly, in order to limit the impact of the phase offset between hops.

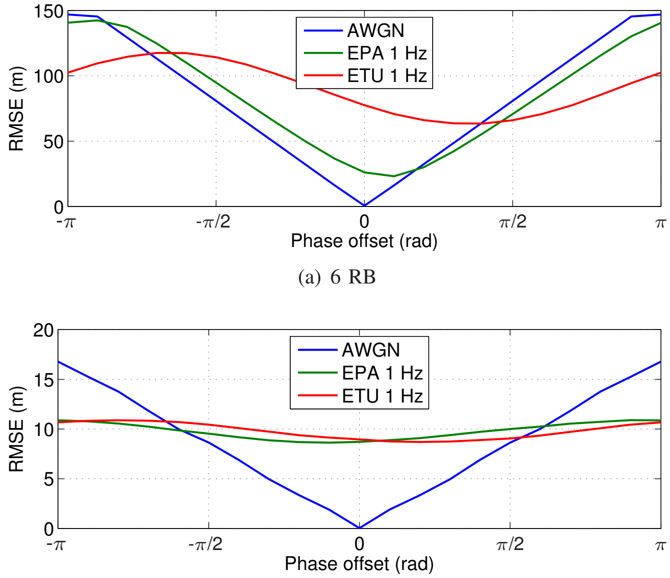

(a) 6 RB

(b) 50 RB

Fig. 6. Impact of the phase offset on the RMSE of the TDE with two hops over 6 and 50 RB for C/N_0 =90 dB-Hz without group delay, i.e., $\Delta_k = 0$, by using 1000 Monter-carlo simulations.

B. Impact on the Positioning Performance

The typical hexagonal cell layout of 7 three-sectorial BSs sites (i.e., 19 hexagonal cells) is considered to evaluate the positioning performance under hop impairments. The inter-site distance is set to 500 meters, and the mobile device position is defined by a grid of equi-spaced points with a resolution of 10 meters within the 19 cells, which results in 15896 positions. The received signal is assumed to have $C/N_0 \geq 90$ dB-Hz, in order to assess ranging errors dominated by multipath and hop impairments. The range estimation is modelled as follows

$$\hat{\tau} = d_{\mathrm{BS}} + \epsilon_{\mathrm{hop}}, \tag{6}$$

where d_{BS} is the distance between BS and mobile device, and ϵ_{hop} is the TDE error obtained with the threshold-based estimation, as in the previous section. For each mobile position, one EPA or ETU channel realisation is computed, and the FH PRS ranging is measured, by considering a group delay of -10 ns and three different definitions of the phase offset, i.e., $\theta_k = 0°$, $\theta_k \sim \mathcal{U}(-20°, 20°)$, and $\theta_k \sim \mathcal{U}(-40°, 40°)$, being $\mathcal{U}(\alpha, \beta)$ a uniform distribution of random values between α and β. The LTE network is assumed to be tightly synchronized, and the inter-cell interference is considered to be avoided by means of a PRS muting mechanism. The TDoA position is then estimated with ranging measurements from four BSs by means of a classical least-squares (LS) algorithm. The resulting cumulative density function (CDF) of the position errors is shown in Figure 7. The positioning results for the 67% of the CDF are summarized in Table II. The phase offset has a noticeable impact on the positioning error, especially for the 6 RB case, as it can be seen with the distributions of phase offset considered in these simulations. This confirms the importance of a FH receiver architecture able to compute coherent TDE between hops. If this hop impairment is ameliorated, the FH PRS scheme is a good NB-IoT candidate method to achieve a position accuracy below 50 meters, with an equivalent bandwidth of 6 and 50 RB for multipath with low and high delay spread, respectively.

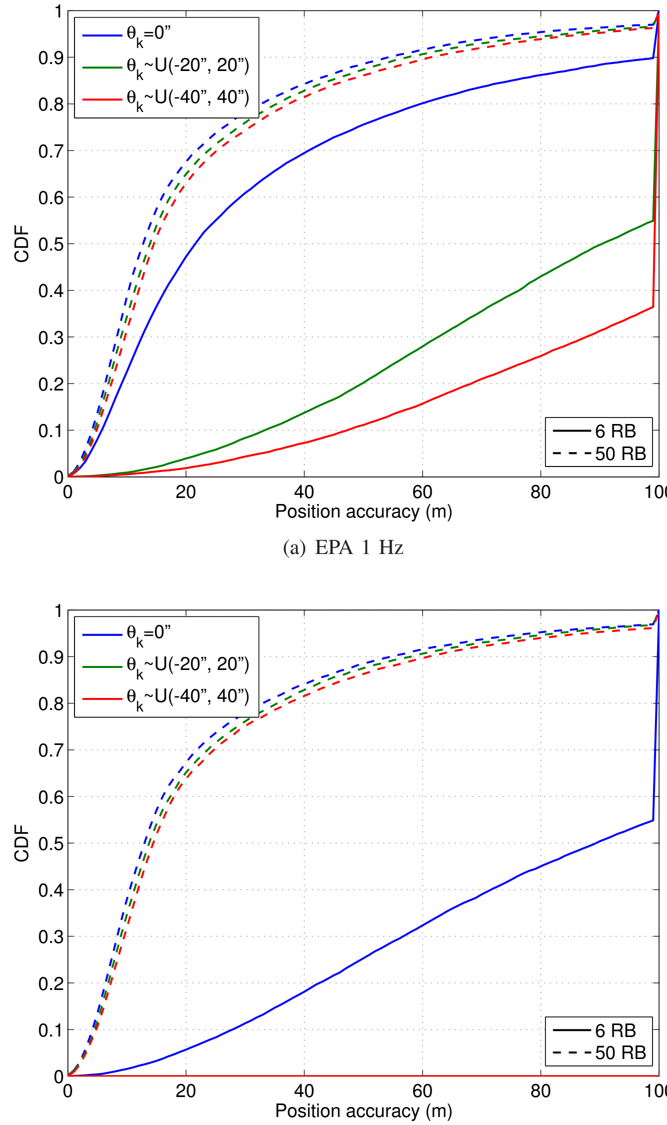

(a) EPA 1 Hz

(b) ETU 1 Hz

Fig. 7. Position accuracy with FH PRS covering a 6-RB and 50-RB signal bandwidth for different phase offset distributions and a group delay of -10 ns.

TABLE II. POSITION ERROR WITH FH PRS AT 67% OF THE CDF.

Channel model	FH PRS bandwidth	Phase offset $0°$	$\mathcal{U}(-20°, 20°)$	$\mathcal{U}(-40°, 40°)$
EPA 1 Hz	6 RB	36.6 m	>100 m	>100 m
	50 RB	19.7 m	21.4 m	22.7 m
ETU 1 Hz	6 RB	>100 m	>100 m	>100 m
	50 RB	19.8 m	21.3 m	22.4 m

The preliminary results of this work indicate the potential of the FH PRS scheme to achieve accurate NB-IoT positioning. However, further research is still necessary to investigate different FH PRS configurations, such as the impact of the integration time, number of hops and hop interval. Thus, future work is aimed to assess these configurations, and to study the introduction of advanced TDE techniques.

VI. Conclusion

This work studies the impact of a frequency-hopping (FH) scheme on the positioning capabilities of the narrowband Internet of things (NB-IoT) technology within Long Term Evolution (LTE) cellular networks, as a predecessor of future fifth generation (5G) networks. This assessment is based on the use of a FH mechanism over the positioning reference signal (PRS). The NB-IoT device coherently estimates the time delay by using the edge resources of an in-band PRS transmission. The ranging performance of this FH PRS mechanism is limited by receiver and channel impairments. The simulation results show a time-difference of arrival (TDoA) position accuracy below 50 meters, by using two frequency hops over a system bandwidth of 10 MHz and dense multipath. Still, the FH receiver architecture may need to be properly designed to limit the hop impairments. Future work is aimed to assess advanced FH PRS configurations for NB-IoT, and to introduce advanced time-delay estimation techniques.

Acknowledgment

This work was supported by the ESA under NPI programme No. 4000110780/14/NL/AK, and by the Spanish Ministry of Science and Innovation project TEC2014-53656-R.

References

[1] A. Zanella, N. Bui, A. Castellani, L. Vangelista, and M. Zorzi, "Internet of things for smart cities," *IEEE Internet of Things Journal*, vol. 1, no. 1, pp. 22–32, Feb 2014.

[2] C. Hoymann, D. Astely, M. Stattin, G. Wikstrom, J. F. Cheng, A. Hoglund, M. Frenne, R. Blasco, J. Huschke, and F. Gunnarsson, "LTE release 14 outlook," *IEEE Communications Magazine*, vol. 54, no. 6, pp. 44–49, June 2016.

[3] R. D. Taranto, S. Muppirisetty, R. Raulefs, D. Slock, T. Svensson, and H. Wymeersch, "Location-Aware Communications for 5G Networks: How location information can improve scalability, latency, and robustness of 5G," *IEEE Signal Processing Magazine*, vol. 31, no. 6, pp. 102–112, Nov 2014.

[4] FCC, "Fourth report and order on wireless E911 location accuracy requirements," Tech. Rep., Jan. 2015.

[5] D. Vasisht, S. Kumar, and D. Katabi, "Decimeter-level localization with a single WiFi access point," in *13th USENIX Symposium on Networked Systems Design and Implementation (NSDI 16)*, 2016, pp. 165–178.

[6] A. Goetz, R. Rose, S. Zorn, G. Fischer, and R. Weigel, "Performance of coherent time delay estimation techniques for frequency hopping GSM signals," in *IEEE Topical Conference on Wireless Sensors and Sensor Networks (WiSNet)*, Jan 2012, pp. 25–28.

[7] R1-166589, "OTDOA positioning in NB-IoT," RAN WG1 #86, Nokia, Alcatel-Lucent Shanghai Bell, Aug. 2016.

[8] R1-1608618, "Design of new downlink positioning reference signal for NB-IoT," RAN WG1 #86, Huawei, HiSilicon, Oct. 2016.

[9] R1-1612602, "OTDOA for NB-IoT," RAN WG1 #87, ZTE, Nov. 2016.

[10] 3GPP TS 36.305, *Stage 2 functional specification of user equipment (UE) positioning in E-UTRAN*, Std., Rel. 13, Dec. 2015.

[11] RP-162520, "Revised work item proposal: Further Enhanced MTC for LTE," RAN #74, Dec. 2016.

[12] R1-1701552, "Final report of 3GPP TSG RAN WG1 #87," MCC Support, RAN WG1 #87, Feb. 2017.

[13] RP-161901, "Revised work item proposal: Enhancements of NB-IoT," RAN #73, Sep. 2016.

[14] RP-161260, "New Work Item Positioning Enhancements for GERAN," RAN #72, June. 2016.

[15] RP-170192, "Status Report: Positioning Enhancements for GERAN," RAN #75, Mar. 2017.

[16] D. Dardari, A. Conti, U. Ferner, A. Giorgetti, and M. Z. Win, "Ranging with ultrawide bandwidth signals in multipath environments," *Proceedings of the IEEE*, vol. 97, no. 2, pp. 404–426, Feb 2009.

[17] W. Xu, M. Huang, C. Zhu, and A. Dammann, "Maximum likelihood TOA and OTDOA estimation with first arriving path detection for 3GPP LTE system," *Trans. Emerging Tel. Tech.*, vol. 27, pp. 339–356, 2016.

[18] A. Dammann, T. Jost, R. Raulefs, M. Walter, and S. Zhang, "Optimizing waveforms for positioning in 5G," in *IEEE 17th International Workshop on Signal Processing Advances in Wireless Communications (SPAWC)*, July 2016, pp. 1–5.

[19] 3GPP TS 36.101, *UE radio transmission and reception*, Std., Rel. 13, Jan. 2016.